THE JOURNAL OF PHYSICAL CHEMISTRY A
A JOURNAL OF THE AMERICAN CHEMICAL SOCIETY

pubs.acs.org/JPCA

Article

Theoretical Characterization of Carbonic Acid Clusters in the UV

Published as part of The Journal of Physical Chemistry virtual special issue "10 Years of the ACS PHYS Astrochemistry Subdivision".

Austin M. Wallace and Ryan C. Fortenberry*

Cite This: *J. Phys. Chem. A* 2022, 126, 3739−3744

Read Online

ACCESS | Metrics & More | Article Recommendations | Supporting Information

ABSTRACT: Two theoretical structural motifs are proposed to match two experimental solid carbonic acid UV spectra from previous literature (*Astron. Astrophys.* **2021**, *646*, A172): a linear ribbon structure as a single octamer and nonplanar orientations of carbonic acid clusters. The latter have some contribution from approximated amorphous solid carbonic acid in the form of 40 different clusters of 8 carbonic acid molecules ensemble-averaged together, but unoptimized pairs of optimized dimers oriented perpendicular to one another give the strongest intensities of lower energy UV transitions. The linear ribbon structure's predicted spectrum computed with CAM-B3LYP/6-311G(d,p) agrees well with Experimental Solid B—the β-carbonic acid experimental data in the UV region. Meanwhile, the 40 amorphous clusters are built with a randomization script, and the electronically excited states are calculated with both CAM-B3LYP/6-311G(d,p) and ωB97XD/6-311G(d,p). The resulting theoretical spectrum is constructed by employing a Boltzmann distribution of the intensities and artificially broadening the simulated spectra. The nonplanar dimer pairs are computed with CAM-B3LYP and B3LYP with the 6-311G(d,p) basis set. The results of the amorphous simulation weakly correspond with the Experimental Solid A spectrum, but the fully nonplanar motif matches the experiment much more convincingly. As a result, the previous work appears to have observed the traditional crystalline phase of solid carbonic acid in Experimental Solid B, whereas the nonplanar orientations of the carbonic acids in the clusters appear to correlate with Experimental Solid A. This spectral classification will aid in future laboratory work exploring the role that carbonic acid can play in low temperature, low pressure desorbed environments with potential application to astrochemistry.

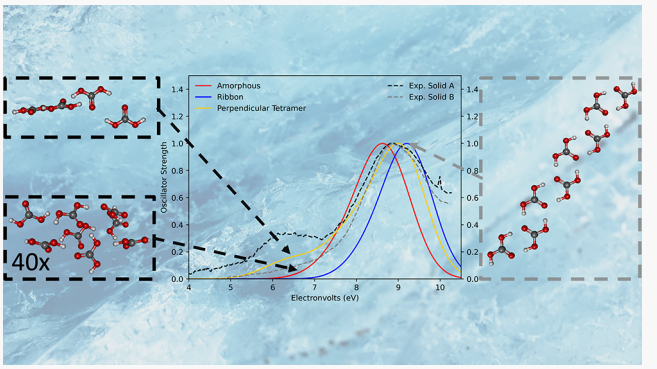

INTRODUCTION

Carbonic acid is believed to exist in various terrestrial environments performing a wide range of functions associated with biology and geology. In a biological context, carbonic acid is believed to serve as a vital component for physiological processes as a weak acid transporting carbon dioxide through the circulatory system.[1] Geologically, carbonic acid is essential in the carbon cycle[2,3] and is hypothesized to be key to the formation of carbonate minerals as the starting material for the ultimate carbon trioxide moiety.[4,5] Although carbonic acid is likely essential for various chemical processes on Earth, no detection of the molecule exists in extraterrestrial environments, and by extension, other key, potential functions of carbonic acid throughout the universe are still unknown.

Even though carbonic acid has not been detected in the interstellar medium (ISM) nor the Solar System, previous work has demonstrated that carbonic acid may form through the irradiation of H_2O-CO_2 ices with ultraviolet (UV) light matching numerous interstellar environmental conditions.[6−9] With the high amounts of H_2O and CO_2 ices throughout the Solar System and ISM, the formation of carbonic acid seems quite likely; still, no detection has been confirmed.[10−16] Therefore, infrared (IR) investigations into identifying carbonic acid have looked for it in various astronomical sources.[17,18] However, because carbonic acid has many overlapping vibrational frequencies with other more abundant species in the solid phase,[8] detection in the Solar System through IR spectroscopy is a challenge leading investigations to favor the UV region. To this end, recent laboratory experimental work has produced solid carbonic acid UV spectra for what has been dubbed Experimental Solid A with unknown structure and its counterpart Experimental Solid B,

Received: February 4, 2022
Revised: May 23, 2022
Published: June 7, 2022

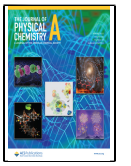

https://doi.org/10.1021/acs.jpca.2c00862
J. Phys. Chem. A 2022, 126, 3739−3744

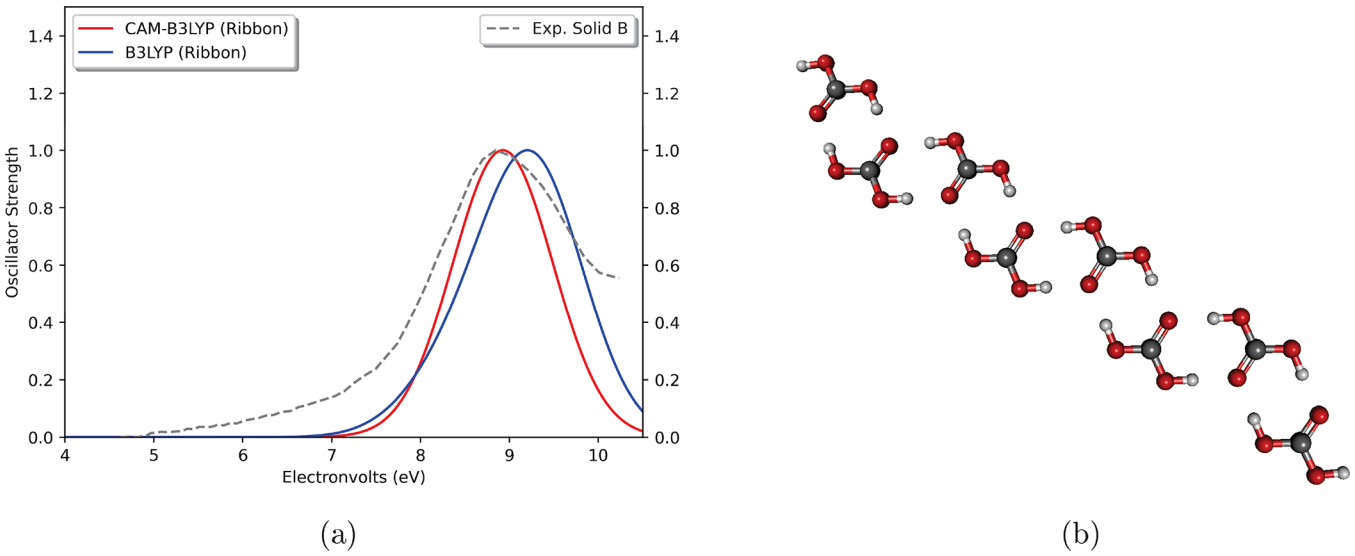

Figure 1. (a) Computed VUV spectra for the carbonic acid ribbon octamer compared to experimental data for Experimental Solid B for H_2CO_3 from ref 8. (b) Ribbon octamer.

which is believed to correspond to the known β-carbonic acid polymorph.[8]

Overall, three polymorphs have been proposed for the solid structures of carbonic acid, but only β-carbonic acid is confirmed to exist.[8,19,20] Early research into solid phase carbonic acid had shown support for α-carbonic acid and β-carbonic acid through the formation under acid−base reactions conducted at low temperatures.[21] However, the formation of α-carbonic acid relies upon the usage of a methanolic solution that actually produces the monomethyl ester of carbonic acid (CH_3OCO_2H), as shown through comparing matrix-isolation IR spectra of both α-carbonic acid and monomethyl ester.[19,22−26] Meanwhile, β-carbonic acid can be produced from the irradiation of CO_2:H_2O ice mixtures raised to the temperature of 220 K.[6,8]

Previous computational work has demonstrated that the lowest energy isomer of the carbonic acid monomers is the *syn-syn* conformation with the hydrogens both pointing toward the ketone oxygen—a unit of β-carbonic acid.[20,27] This monomer is followed closely in relative energy by the *syn-anti* conformational isomer at 0.08 eV higher in energy. The *anti-anti* conformational isomer is substantially higher in energy at 0.49 eV higher than the *syn-syn* isomer.[20,28] Furthermore, computational and experimental investigations into the β-carbonic acid polymorph support the idea that the structure is composed of *syn-syn* carbonic acid monomers linked together in a ribbon structure.[20,27−29] In the UV region, β-carbonic acid is characterized by a single major peak at 8.92 eV (139 nm).[8] Finally, another carbonic acid solid has appeared in literature through the formation of carbonic acid through a radical reaction between CO and OH in a watery environment at low temperatures (10−40 K).[18,26,30] The defining feature for this form of carbonic acid (Experimental Solid A) comes from a minor peak at approximately 6.2 eV (200 nm) on the shoulder of the 8.92 eV feature; however, theoretical work has yet to describe the carbonic acid structure responsible for this peak in the UV region. The present work aims to achieve this.

Simultaneously, a new procedure leveraging quantum mechanics and statistical mechanics has been able to generate UV spectra for amorphous water, ammonia, and carbon dioxide in agreement with experiment with a mean absolute error of 3.3% for CAM-B3LYP/6-311G(d,p).[31] Such a procedure is related to ongoing research in polymolecular quantum chemistry,[32,33] and this represents an extension to amorphous solids of astrophysical application.[20,31] Therefore, the present work will utilize this procedure to analyze amorphous carbonic acid clusters' UV spectra to potentially characterize the unknown carbonic acid structure observed in Experimental Solid A.[8] Additionally, the ribbon structure is investigated further with respect to the Experimental Solid B spectrum, and a new twisted motif for pairs of dimers is also explored to see its relevance to either case. A helical motif of optimized carbonic acid clusters has also been reported recently,[20] but its role in the observed spectra has yet to be determined. These combined analyses will be able to provide novel insights into the UV spectrum of carbonic acid in the solid phase where its presence in simulated extraterrestrial ices may yet be confirmed.

COMPUTATIONAL METHODS

Amorphous carbonic acid is simulated by generating 40 randomized clusters.[31] Each cluster consists of 8 carbonic acid molecules composed of the two lowest energy conformational isomers of the monomer. Previous work has shown that 8 carbonic acid molecules are enough to achieve convergence in the spectra,[20] and the same number produces similar behavior in related carbon dioxide clusters.[31] Although 30 clusters are composed of the lowest energy *syn-syn* carbonic acid monomers, 5 clusters are built from the second lowest conformational isomer, *syn-anti* monomers, and the remaining 5 clusters are a mixture of *syn-syn* and *syn-anti* monomers. Incorporating some of the *syn-anti* monomers provides a more complete sampling of the amorphous structure. Then, each cluster is optimized with ωB97-XD/6-31G(d)[34−36] with Gaussian16[37] with the energies stored for use in the Boltzmann distribution. Next, the optimized cluster structures are used to calculate the electronically excited states with time-dependent density functional theory (TD-DFT) via the CAM-B3LYP,[38−41] B3LYP, and ωB97-XD[42] methods conjoined to the 6-311G(d,p) basis set[35,36] for 25 excited states, because 25

https://doi.org/10.1021/acs.jpca.2c00862
J. Phys. Chem. A 2022, 126, 3739−3744

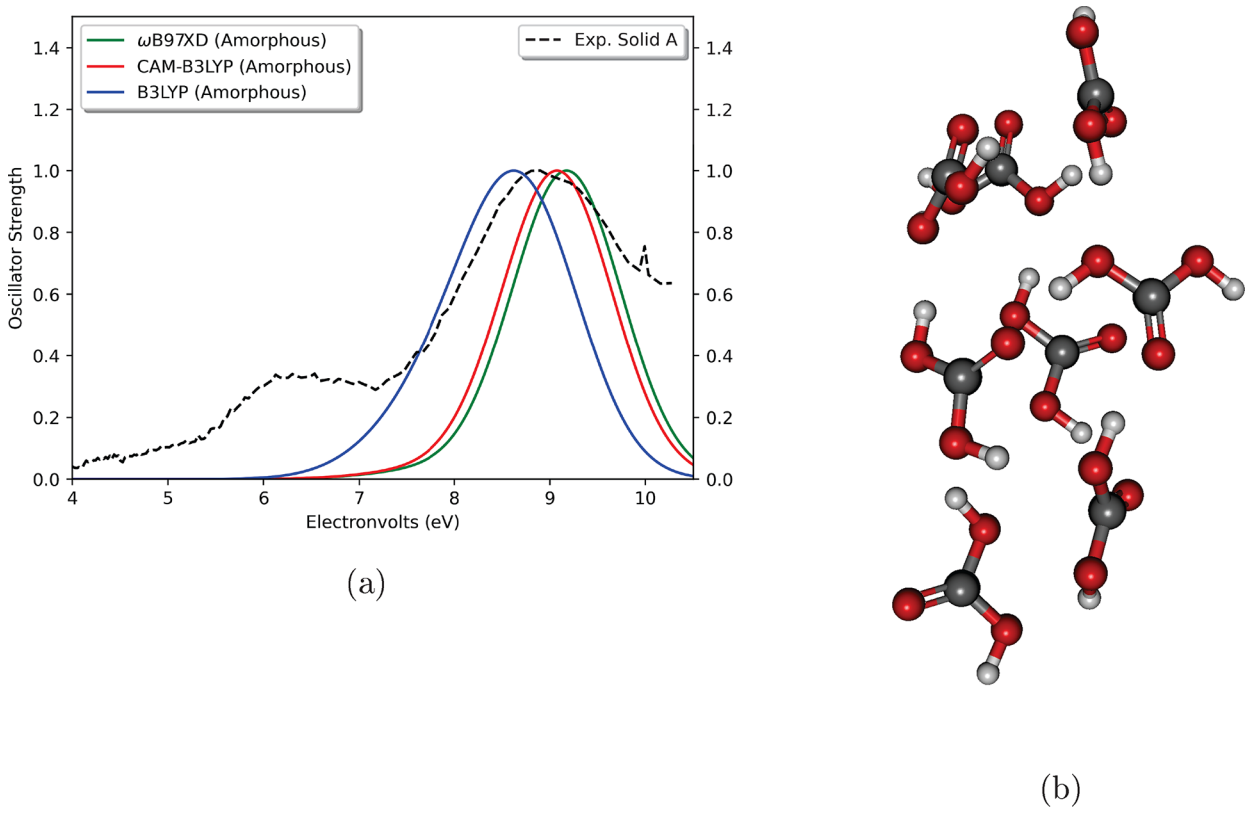

Figure 2. (a) Computed VUV spectra for 40 clusters of 8 carbonic acid molecules compared with experiment from ref 8. (b) Lowest energy cluster depicted from the 40 used to build the spectrum.

states cover the main features observed in the experimental spectra. To predict the spectrum of a larger, bulk amorphous solid, each isomer's excited states' oscillator strengths are scaled by a Boltzmann factor. This factor is produced for each cluster from relative energies to mimic the relative abundances of each cluster's contribution in an amorphous solid ice. By approximation of all the binding energy turning into the thermal energy, the temperature for calculating the Boltzmann factor comes from the binding energy of the lowest energy dimer (0.80 eV),[20] yielding 9259 K. The full set of scaled excitations are input into a Gaussian line shape procedure with a full width at half-maximum height of 0.5 eV, which constructs a normalized artificial UV spectrum. Again, a similar procedure has been shown to reproduce the UV experimental spectrum of amorphous ammonia, carbon dioxide, and water in a semiquantitative fashion such that unique interpretation of the experimental results based on the theoretical results is possible.

The linear octamer ribbon structure is the extended structure from previous work that appears to correspond with β-carbonic acid.[20,27] This octamer is optimized with ωB97-XD/6-31G(d), and the electronically excited states are calculated with CAM-B3LYP/6-311G(d,p) with 15 states and B3LYP/6-311G(d,p) with 100 states. The number of excited states are increased to reach approximately 9.5 eV to compare more appropriately with experiment. The perpendicular motif composed of unoptimized pairs of optimized dimers where the dihedral angles of pairs of ribbin dimers are now at roughly 90°. These structures are computed with 40 electronic states from CAM-B3LYP/6-311G(d,p) and ωB97-XD/6-311G(d,p) as well as B3LYP/6-311G(d,p) with 80 states. All of the simulated carbonic acid clusters results are compared with experimental data on what is reported to be solid carbonic acid from previous work presented in Figure 6 of Ioppolo et al.[8]

RESULTS AND DISCUSSION

The UV spectrum for the linear octamer ribbon structure is depicted against the experimental solid B in Figure 1.[8] The Experimental Solid B plot comes from work done by Ioppolo et al. in which solid carbonic acid is formed at 80 K, annealed to 225 K and cooled to 80 K. The computed electronically excited states with CAM-B3LYP show high qualitative and even quantitative agreement through having a single major peak at 8.90 eV, which is notably close to the experimental value of 8.92 eV (139 nm).[20,27] This supports previous claims that the ribbon structure corresponds too Experimental Solid B and, by extension, β-carbonic acid through spectral agreement in the UV region.

The 40 carbonic acid clusters simulating an amorphous solid produce the UV spectrum in Figure 2 with two major peaks for both CAM-B3LYP and ωB97XD. The relative energies for these clusters are contained in the Supporting Information. These depictions qualitatively match Experimental Solid A.[8] The Experimental Solid A plot also comes from work done by Ioppolo et al. in which solid carbonic acid is formed at 20 K, annealed to 225 K, and cooled to 20 K. CAM-B3LYP and ωB97XD both depict the largest peak around 9 eV (9.07 and 9.17, respectively) corresponding to the dominant experimental peak at 8.92 eV.[8] The source of this excitation is from a nonbonding molecular orbital (MO) into a π^* MO in the external carbonic acid molecules. This is the same feature as that present in the linear, ribbon structure discussed above.

The UV spectrum for Experimental Solid A differs from Experimental Solid B by having an additional peak at 6.27 eV

https://doi.org/10.1021/acs.jpca.2c00862
J. Phys. Chem. A 2022, 126, 3739−3744

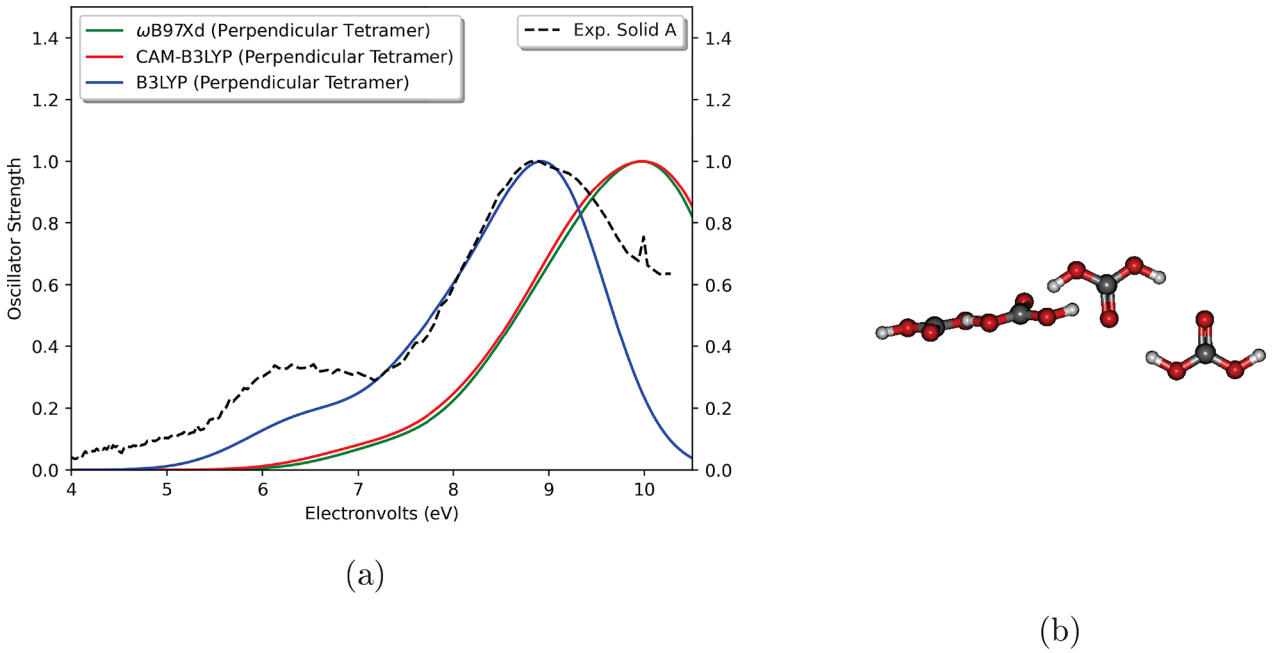

Figure 3. (a) Computed VUV spectra for the perpendicular tetramer of carbonic acid compared with experiment from ref 8. (b) Structure of the perpendicular tetramer.

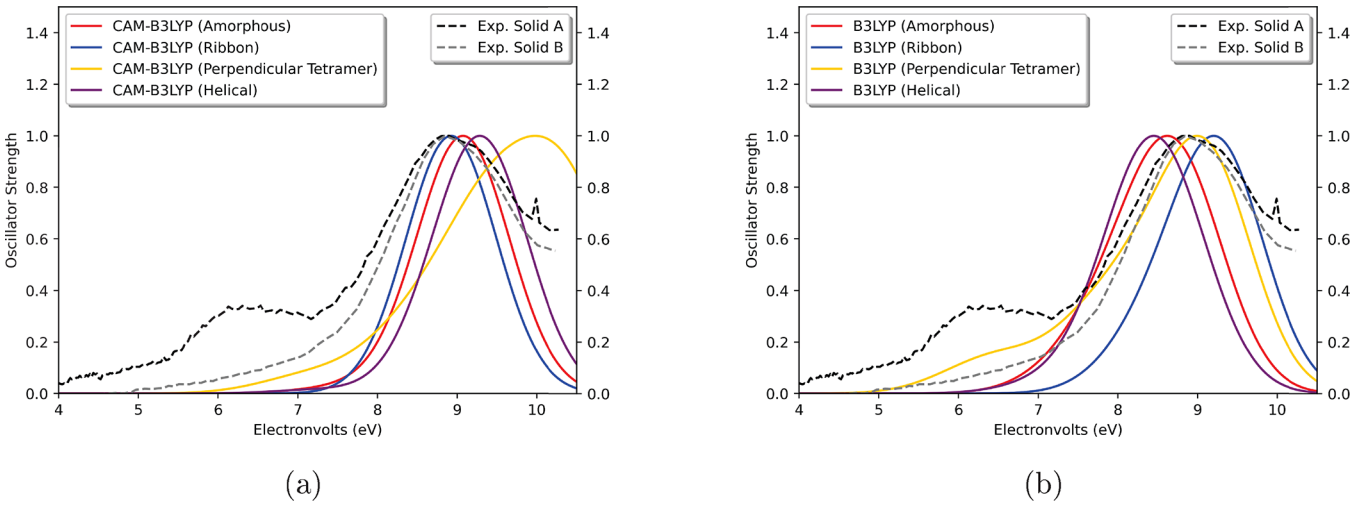

Figure 4. Computed VUV spectra of amorphous, helical, perpendicular, and ribbon carbonic acid clusters calculated with CAM-B3LYP (A) and B3LYP (B) compared with Experimental Solid A and B results from ref 8.

(198 nm).[8] The computational spectrum for CAM-B3LYP and ωB97XD for clusters of amorphous carbonic acid both predict a secondary peak, as well, appearing at 7.38 and 7.41 eV, respectively, coming from an excitation starting once again in a nonbonding MO but promoting the electron into a σ^* MO. This excitation is also present in the ribbon structure, but the symmetry of the ribbon forces this excitation to have a zero oscillator strength. The amorphous simulations have C_1 symmetry, which allows these excitations to produce nonzero (albeit still relatively small) oscillator strengths for these lower energy excitations. Only semiquantitative agreement exists between the amorphous solid and the Experimental Solid A because the computed excitations are approximately 1 eV away. From previous benchmarking on clusters with 8 molecules and CAM-B3LYP/6-311G(d,p), the amorphous spectra predictions for water, ammonia, and carbon dioxide are off from experiment by 0.51, 0.32, and 0.24 eV, respectively.[31] Though such a shift could put the amorphous style clusters more in line with the experiments, such would still likely fall short. However, the amorphous clusters do provide a possible clue as to the origins of lower energy feature in their nonzero oscillator strength n → σ^* transitions.

Figure 3 provides an additional possibility for the cause of the secondary UV feature in the 5.5−7.3 eV range: perpendicular clusters. In a test of various tetramers composed of unoptimized pairs of optimized dimers, the near-perpendicular orientation of the two dimer pairs maximizes signal from the n → σ^* transitions. Although the oscillator strengths of the individual excited states are on the order of 10^{-1} or less, these are orders of magnitude more than the n → σ^* oscillator strengths in the amorphous clusters, and there are numerous excitations from the perpendicular dimers in this energy regime. These constructively add together to give the spectrum in Figure 3. Interestingly, the B3LYP perpendicular

https://doi.org/10.1021/acs.jpca.2c00862
J. Phys. Chem. A 2022, 126, 3739−3744

tetramer computations nearly perfectly match the Experimental Solid A spectrum. The CAM-B3LYP and ωB97-XD computations are much more consistent with one another and predict the secondary peak to be at a similar energy as the secondary peak from the computed UV spectrum of the amorphous cluster. However, these two functionals have the major peak higher in energy than the experimental major peak and also showcase that the secondary peak is roughly 3 eV less than the main peak is present as is exhibited in Experimental Solid A. As a result, if CAM-B3LYP is overestimating the excitation energy and B3LYP is closer to physical reality, then the present, secondary peak likely arises from this perpendicular arrangement of carbonic acid molecules. Although these pairs of dimers ultimately optimize to the ribbon structure when left to minimize,[20] this perpendicular motif may be present in the carbonic acid observed experimentally at any given time in enough concentration to produce the secondary, red-shifted UV peak in Experimental Solid A.

Figure 4 brings together the best theoretical data with the experimental data from ref 8 to display the unique differences between the forms of carbonic acid experimentally produced and those computationally analyzed with both B3LYP and CAM-B3LYP. Though both the ribbon and amorphous structures have a major peak at approximately 9 eV for both levels of theory, the lack of symmetry in the amorphous and helical[20] clusters allows the nonbonding to σ^* excitation to exhibit some oscillator strength that the C_{2v} and C_{2h} ribbon structures forbid. This continues to a much greater extent in the perpendicular motif. The lower energy UV feature for Experimental Solid A is likely the result of n $\rightarrow$ σ^* transitions for nonplanar carbonic acid clusters. The optimized amorphous clusters begin to show this property, and this is even exposed in the helix form discussed previously.[20] However, the oscillator strengths of these transitions appear to be somewhat maximized once the dimers are oriented perpendicular to one another. The functionals examined here provide differing energies for the major peak, but both show that the perpendicular tetramer is still the only one that has notable spectral features lower in energy than the major peak.

CONCLUSIONS

The UV spectrum for carbonic acid appears to have two competing characterizations, split into Experimental Solid A and B. Computationally, the linear octamer ribbon structure matches the Experimental Solid B, further strengthening the claim that the ribbon is responsible for the β-carbonic acid polymorph. Meanwhile, Experimental Solid A is characterized by having two major peaks with the smaller peak arising on the lower energy side, which maps to the computationally predicted spectrum of carbonic acid clusters with molecules oriented out of the plane from one another. Though the currently computed amorphous and the previously computed helical clusters demonstrate this behavior to some extent,[20] the perpendicular pairs of optimized dimers clearly showcase the relatively strong transitions in the needed 5.5−7.3 eV range. Hence, this perpendicular orientation motif is likely present in the Experimental Solid A reported in ref 8. As a result, the lower temperature (20 K), Experimental Solid A irradiation appears to contain the nonplanar motif, whereas the higher temperature (80 K) irradiation does not. The lower temperatures appear to conserve the nonplanar motif of the carbonic acid whereas the higher temperature environment does not allow for its production. The exact form of the carbonic acid in Experimental Solid A is still unclear and will be pursued in future work, but the nonplanarity of the clusters in a near-perpendicular arrangement is seemingly required for the spectra associated with Experimental Solid A.

ASSOCIATED CONTENT

Supporting Information

The Supporting Information is available free of charge at https://pubs.acs.org/doi/10.1021/acs.jpca.2c00862.

Cluster relative energies and carbonic acid clusters' Cartesian coordinates (PDF)

AUTHOR INFORMATION

Corresponding Author

Ryan C. Fortenberry − *Department of Chemistry & Biochemistry, University of Mississippi, University, Mississippi 38677-1848, United States;* orcid.org/0000-0003-4716-8225; Email: r410@go.olemiss.edu

Author

Austin M. Wallace − *Department of Chemistry & Biochemistry, University of Mississippi, University, Mississippi 38677-1848, United States;* orcid.org/0000-0002-0659-6912

Complete contact information is available at: https://pubs.acs.org/10.1021/acs.jpca.2c00862

Notes

The authors declare no competing financial interest.

ACKNOWLEDGMENTS

This work is supported by NSF Grant OIA-1757220, NASA Grant NNX17AH15G, and the University of Mississippi. A.M.W. acknowledges support from the Sally McDonnell Barksdale Honors College at the University of Mississippi as well as the Barry Goldwater Scholarship & Excellence in Education Foundation. Finally, the authors thank Prof. Ralf I. Kaiser of the University of Hawaii for useful conversations related to this work.

REFERENCES

(1) Pines, D.; Ditkovich, J.; Mukra, T.; Miller, Y.; Kiefer, P. M.; Daschakraborty, S.; Hynes, J. T.; Pines, E. How Acidic is Carbonic Acid? *J. Phys. Chem. B* **2016**, *120*, 2440−2451.

(2) Stolte, N.; Pan, D. Large Presence of Carbonic Acid in CO_2-Rich Aqueous Fluids Under Earth's Mantle Conditions. *J. Phys. Chem. Lett.* **2019**, *10*, 5135−5141.

(3) Li, C.; Ji, H. Chemical Weathering and the Role of Sulfuric and Nitric Acids in Carbonate Weathering: Isotopes (13C, 15N, 34S, and 18O) And Chemical Constraints. *Journal of Geophysical Research: Biogeosciences* **2016**, *121*, 1288−1305.

(4) Kanakiya, S.; Adam, L.; Esteban, L.; Rowe, M. C.; Shane, P. Dissolution and Secondary Mineral Precipitation in Basalts due to Reactions with Carbonic Acid. *Journal of Geophysical Research: Solid Earth* **2017**, *122*, 4312−4327.

(5) Abbaszadeh, M.; Nasiri, M.; Riazi, M. Experimental Investigation of the Impact of Rock Dissolution on Carbonate Rock Properties in the Presence of Carbonated Water. *Environmental Earth Sciences* **2016**, *75*, 791.

(6) Zheng, W.; Kaiser, R. I. On The Formation of Carbonic Acid (H_2CO_3) in Solar System Ices. *Chem. Phys. Lett.* **2007**, *450*, 55−60.

(7) Moore, M.H.; Khanna, R.K. Infrared and Mass Spectral Studies of Proton Irradiated H_2O + CO_2 Ice: Evidence for Carbonic Acid.

Spectrochimica Acta Part A: Molecular Spectroscopy **1991**, *47*, 255−262.
(8) Ioppolo, S.; Kanuchová, Z.; James, R. L.; Dawes, A.; Ryabov, A.; Dezalay, J.; Jones, N. C.; Hoffmann, S. V.; Mason, N. J.; Strazzulla, G. Vacuum Ultraviolet Photoabsorption Spectroscopy of Space-Related Ices: Formation and Destruction of Solid Carbonic Acid Upon 1 KeV Electron Irradiation. *Astronomy & Astrophysics* **2021**, *646*, A172.
(9) Jones, B. M.; Kaiser, R. I.; Strazzulla, G. Carbonic Acid as a Reserve of Carbon Dioxide on Icy Moons: The Formation of Carbon Dioxide (CO_2) in a Polar Environment. *Astrophysical Journal* **2014**, *788*, 170.
(10) Radhakrishnan, S.; Gudipati, M. S.; Sander, W.; Lignell, A. Photochemical Processes in CO2/H_2O Ice Mixtures with Trapped Pyrene, a Model Polycyclic Aromatic Hydrocarbon. *Astrophysical Journal* **2018**, *864*, 151.
(11) Gerakines, P. A.; Whittet, D. C. B.; Ehrenfreund, P.; Boogert, A. C. A.; Tielens, A. G. G. M.; Schutte, W. A.; Chiar, J. E.; van Dishoeck, E. F.; Prusti, T.; Helmich, F. P.; et al. Observations of Solid Carbon Dioxide in Molecular Clouds with the Infrared Space Observatory. *Astrophysical Journal* **1999**, *522*, 357−377.
(12) Boogert, A. A.; Gerakines, P. A.; Whittet, D. C. Observations of the Icy Universe. *Annual Review of Astronomy and Astrophysics* **2015**, *53*, 541−581.
(13) Hoang, M.; Altwegg, K.; Balsiger, H.; Beth, A.; Bieler, A.; Calmonte, U.; Combi, M. R.; De Keyser, J.; Fiethe, B.; Fougere, N.; et al. The Heterogeneous Coma of Comet 67p/Churyumov-Gerasimenko as Seen by Rosina: H_2O, CO_2, and CO from September 2014 to February 2016. *Astron. Astrophys.* **2017**, *600*, A77.
(14) Buratti, B. J.; Cruikshank, D. P.; Brown, R. H.; Clark, R. N.; Bauer, J. M.; Jaumann, R.; McCord, T. B.; Simonelli, D. P.; Hibbitts, C. A.; Hansen, G. B.; et al. Cassini Visual And Infrared Mapping Spectrometer Observations of Iapetus: Detection of CO_2. *Astrophysical Journal* **2005**, *622*, L149−L152.
(15) Filacchione, G.; Raponi, A.; Capaccioni, F.; Ciarniello, M.; Tosi, F.; Capria, M. T.; De Sanctis, M. C.; Migliorini, A.; Piccioni, G.; Cerroni, P.; et al. Seasonal Exposure of Carbon Dioxide Ice on The Nucleus of Comet 67p/Churyumov-Gerasimenko. *Science* **2016**, *354*, 1563−1566.
(16) Kuroda, T.; Medvedev, A. S.; Kasaba, Y.; Hartogh, P. Carbon Dioxide Ice Clouds, Snowfalls, and Baroclinic Waves in The Northern Winter Polar Atmosphere of Mars. *Geophys. Res. Lett.* **2013**, *40*, 1484−1488.
(17) Bernard, J.; Seidl, M.; Kohl, I.; Liedl, K. R.; Mayer, E.; Gálvez, O.; Grothe, H.; Loerting, T. Spectroscopic Observation of Matrix-Isolated Carbonic Acid Trapped from the Gas Phase. *Angew. Chem., Int. Ed.* **2011**, *50*, 1939−1943.
(18) Oba, Y.; Watanabe, N.; Kouchi, A.; Hama, T.; Pirronello, V. Formation of Carbonic Acid (H_2CO_3) by Surface Reactions of Non-Energetic OH Radicals with CO Molecules at Low Temperatures. *Astrophysical Journal* **2010**, *722*, 1598−1606.
(19) Reisenauer, H. P.; Wagner, J. P.; Schreiner, P. R. Gas-Phase Preparation of Carbonic Acid and its Monomethyl Ester. *Angew. Chem., Int. Ed.* **2014**, *53*, 11766−11771.
(20) Wallace, A. M.; Fortenberry, R. C. Linear And Helical Carbonic Acid Clusters. *J. Phys. Chem. A* **2021**, *125*, 4589−4597.
(21) Hage, W.; Hallbrucker, A.; Mayer, E. Carbonic Acid: Synthesis by Protonation of Bicarbonate and FTIR Spectroscopic Characterization via a New Cryogenic Technique. *J. Am. Chem. Soc.* **1993**, *115*, 8427−8431.
(22) Dibenedetto, A.; Aresta, M.; Giannoccaro, P.; Pastore, C.; Pápai, I.; Schubert, G. On the Existence of the Elusive Monomethyl Ester of Carbonic Acid [$CH_3OC(O)OH$] at 300 K: ^{1}H-and ^{13}C NMR Measurements and DFT Calculations. *Eur. J. Inorg. Chem.* **2006**, *2006* (5), 908−913.
(23) Wagner, J. P.; Reisenauer, H. P.; Hirvonen, V.; Wu, C.-H.; Tyberg, J. L.; Allen, W. D.; Schreiner, P. R. Tunnelling in carbonic acid. *Chem. Commun.* **2016**, *52*, 7858−7861.
(24) Linden, M. M.; Wagner, J. P.; Bernhardt, B.; Bartlett, M. A.; Allen, W. D.; Schreiner, P. R. Intricate Conformational Tunneling in Carbonic Acid Monomethyl Ester. *J. Phys. Chem. Lett.* **2018**, *9*, 1663−1667.
(25) Barnes, A.; Orville-Thomas, W.; Gaufres, R.; Müller, A. *Matrix isolation spectroscopy*; Springer Science & Business Media, 2012; Vol. *76*.
(26) Köck, E.-M.; Bernard, J.; Podewitz, M.; Dinu, D. F.; Huber, R. G.; Liedl, K. R.; Grothe, H.; Bertel, E.; Schlögl, R.; Loerting, T. Alpha-Carbonic Acid Revisited: Carbonic Acid Monomethyl Ester as a Solid and its Conformational Isomerism in the Gas Phase. *Chemistry − A European Journal* **2020**, *26*, 285−305.
(27) Reddy, S. K.; Balasubramanian, S. Carbonic Acid: Molecule, Crystal and Aqueous Solution. *Chem. Commun.* **2014**, *50*, 503−514.
(28) Murillo, J.; David, J.; Restrepo, A. Insights into the Structure and Stability of the Carbonic Acid Dimer. *Phys. Chem. Chem. Phys.* **2010**, *12*, 10963−10970.
(29) Reddy, S. K.; Kulkarni, C. H.; Balasubramanian, S. Theoretical investigations of Candidate Crystal Structures for β-Carbonic Acid. *J. Chem. Phys.* **2011**, *134*, 124511.
(30) Oba, Y.; Watanabe, N.; Kouchi, A.; Hama, T.; Pirronello, V. Experimental Study of CO_2 Formation by Surface Reactions of Non-Energetic OH Radicals with CO Molecules. *Astrophysical Journal* **2010**, *712*, L174−L178.
(31) MWallace, A. M.; Fortenberry, R. C. Computationl UV Spectra for Amorphous Solids of Small Molecules. *Phys. Chem. Chem. Phys.* **2021**, *23*, 24413−24420.
(32) Giovannini, T.; Egidi, F.; Cappelli, C. Molecular spectroscopy of aqueous solutions: a theoretical perspective. *Chem. Soc. Rev.* **2020**, *49*, 5664−5677.
(33) Uribe, L.; Gómez, S.; Giovannini, T.; Egidi, F.; Restrepo, A. An efficient and robust procedure to calculate absorption spectra of aqueous charged species applied to NO_2^-. *Phys. Chem. Chem. Phys.* **2021**, *23*, 14857−14872.
(34) Chai, J.-D.; Head-Gordon, M. Long-Range Corrected Hybrid Density Functionals with Damped Atom−Atom Dispersion Corrections. *Phys. Chem. Chem. Phys.* **2008**, *10*, 6615−6620.
(35) McLean, A. D.; Chandler, G. S. Contracted Gaussian Basis Sets for Molecular Calculations. I. Second Row Atoms, z = 11−18. *J. Chem. Phys.* **1980**, *72*, 5639−5648.
(36) Krishnan, R.; Binkley, J. S.; Seeger, R.; Pople, J. A. Self-Consistent Molecular Orbital Methods. XX. A Basis Set for Correlated Wave Functions. *J. Chem. Phys.* **1980**, *72*, 650−654.
(37) Frisch, M. J.; Trucks, G. W.; Schlegel, H. B.; Scuseria, G. E.; Robb, M. A.; Cheeseman, J. R.; Scalmani, G.; Barone, V.; Petersson, G. A.; Nakatsuji, H.; et al. *Gaussian 16*, Revision C.01; Gaussian Inc.: Wallingford, CT, 2016.
(38) Yanai, T.; Tew, D. P.; Handy, N. C. A New Hybrid Exchange−Correlation Functional Using The Coulomb-Attenuating Method (CAM-B3LYP). *Chem. Phys. Lett.* **2004**, *393*, 51−57.
(39) Becke, A. D. Density-Functional Thermochemistry. III. The Role of Exact Exchange. *J. Chem. Phys.* **1993**, *98*, 5648−5652.
(40) Yang, W. T.; Parr, R. G.; Lee, C. T. Various Functionals for the Kinetic Energy Density of an Atom or Molecule. *Phys. Rev. A* **1986**, *34*, 4586−4590.
(41) Lee, C.; Yang, W. T.; Parr, R. G. Development of the Colle-Salvetti Correlation-Energy Formula into a Functional of the Electron Density. *Phys. Rev. B* **1988**, *37*, 785−789.
(42) Matsumoto, M.; Nishimura, T. Mersenne Twister: A 623-Dimensionally Equidistributed Uniform Pseudo-Random Number Generator. *ACM Transactions on Modeling and Computer Simulation* **1998**, *8*, 3−30.

https://doi.org/10.1021/acs.jpca.2c00862
J. Phys. Chem. A 2022, 126, 3739−3744